Test and Improvement of 1D Routing Algorithms for Dam-Break Floods

Marcos C. Palu, Ph.D.[1]; and Pierre Y. Julien, M.ASCE[2]

Abstract: Classical models for one-dimensional (1D) flood routing calculations were tested in a synthetic benchmark and in a real dam break case, the observed flashy hydrographs on the Doce River after the collapse of the Fundão Tailings Dam in Brazil. The application of existing methods presented unsatisfactory results, with an error in prediction of the peak discharge up to −18%, and differences in timing to peak up to 4 h. An improved 1D flood routing approach is proposed, solving the dynamic equation into an equivalent linear diffusive wave format. This modified method reformulates the hydraulic diffusion coefficient in terms of the Froude number and flood wave celerity, which are parameters more coherent with the linear model assumption and provide more realistic flood wave attenuation. The solution given by this approach can be carried out using the Crank Nicolson or QUICKEST schemes. The relative percent difference (RPD) in predicted peak discharge is reduced to less than −0.1%. **DOI: 10.1061/(ASCE)HY.1943-7900.0001755.** © *2020 American Society of Civil Engineers.*

Author keywords: Saint-Venant equations; Flood wave propagation; Dam break; Doce river; Fundão tailings dam.

Introduction

Recent extreme flood events from dam breaks highlight the importance of using proper modeling algorithms to simulate flood wave propagation. The threat of a flood downstream from the Oroville Dam in California after the damage on the spillway resulted in a mandatory preventive evacuation order in the cities of Oroville and surrounding areas, which affected 188,000 people (USSD 2018). In 2018, two cases of dam failure: (1) the Saddle Dam D, part of the Xe-Pian Xe-Namnoy hydroelectric power project in Laos; and (2) the Swar Creek Dam in Myanmar impacted tens of thousands of people (BBC 2018; Reuters 2018). In March 2019, heavy storms caused severe floods in the Niobrara River, a tributary of the Missouri River in Nebraska, resulting in the failure of the Spencer Dam (Dolce 2019).

Knowledge about the propagation of large floods affecting the safety of riparian communities requires proper flood routing modeling. Flood routing is defined as the procedure to determine the time and magnitude of flood hydrographs at a point on a watercourse from known hydrographs at one or more points upstream (Chow 1988). However, a simple, robust, and accurate model is still a matter of research (Ostad-Ali-Askari and Shayannejad 2016; Perdikaris et al. 2018).

In order to solve the governing equations of unsteady flow in open channels, several commercial codes have been developed using the finite-difference method (FDM), the finite-volume method (FVM), and the finite-element methods (FEM) (Rowinski and Radecki-Pawlik 2015). For three-dimensional (3D) analyses, some of the available finite-volume-based models are the Flow3D (Flow Science 2019) and ANSYS Fluent (ANSYS 2019), while another option is to use Delft3D-FLOW (Deltares 2019) based on the FDM. These are powerful tools for the simulation of floods in the vicinity of a dam after failure; however, due to computational demand, simplified two-dimensional (2D) and 1D formulations are preferred for the evaluation of flood wave propagation in long river reaches.

The depth-averaged approximation leads to 2D models, and commercial software includes the finite-volume HEC-RAS (USACE 2016c) and SRH-2D (USBR 2017), the finite-difference FLO-2D (FLO-2D 2019) and MIKE 21 (DHI 2019), and the finite-element TELEMAC-2D (TELEMAC 2019). However, despite the gain in popularity of these 2D models, the 1D models are still extensively used for long river reaches (Pilotti et al. 2014). It can be attributed to the acquaintance of the practitioners with the 1D modeling, the simpler computational and implementation procedures, and the availability of detailed data to run 2D models, which can be difficult and expensive to obtain in remote areas (Pilotti et al. 2014). Moreover, the computational demand of 2D models is still high when compared to 1D models. Examples of common commercial 1D finite-difference models are the HEC-RAS (USACE 2016d), SRH-1D (USBR 2018), FLDWAVE (Sylvestre et al. 2010), and MIKE 11(DHI 2017). One can observe that despite the advantages of the finite-volume approach, which are physically derived preserving the conservation laws when compared to the finite-differences (nonconservative approach), 1D commercial codes based on finite-volume are still rarely found.

Flood routing can be calculated using the hydrologic (lumped) or the hydraulic (distributed) approach. Hydrologic routing generally considers the solution of the conservation of mass equation and a relation of storage and discharge in a stream reach or reservoir. In contrast, hydraulic routing is based on solutions of the equations of conservation of momentum and mass (USDA 2014), known as the Saint-Venant or 1D shallow water equations (Zijlema 2015).

For 1D hydraulic finite-difference models, one of the most widespread schemes to solve the Saint-Venant equations in commercial codes is the Preissmann scheme (Zijlema 2015; Battjes and Labeur 2017), also called the four-point implicit method, the box model or scheme, the Preissmann-Cunge or the Sogreah implicit method (Chanson 2004). One should note that the software for

[1]Postdoctoral, Dept. of Civil and Environmental Engineering, Colorado State Univ., Fort Collins, CO 80523 (corresponding author). ORCID: https://orcid.org/0000-0002-6132-7125. Email: marcos.palu@colostate.edu; marcos.palu19@alumni.colostate.edu

[2]Professor, Dept. of Civil and Environmental Engineering, Colorado State Univ., Fort Collins, CO 80523. Email: pierre@engr.colostate.edu

Note. This manuscript was submitted on November 14, 2018; approved on December 3, 2019; published online on April 8, 2020. Discussion period open until September 8, 2020; separate discussions must be submitted for individual papers. This paper is part of the ***Journal of Hydraulic Engineering***, © ASCE, ISSN 0733-9429.

1D flood routing simulation provided by two of the main US agencies responsible for dam operations and safety, the USACE (HEC-RAS) and Bureau of Reclamation (SRH-1D), uses the Preissmann scheme. For this reason, this scheme can be considered a standard practice in the US and worldwide.

Simplified forms of the Saint-Venant equations known as the diffusive wave model can be solved by other numerical schemes, including Crank Nicolson or QUICKEST (Szymkiewicz 2010; Battjes and Labeur 2017; Julien 2018). An alternative approach is to apply simpler models such as the Muskingum–Cunge method, which is recommended by the Montana Dam Safety Program for flood routing calculations in natural channels after dam breaks (DNRC 2018).

In this article, different flood routing models–three diffusive wave models and one dynamic wave model–are first tested against a synthetic benchmark, and then applied to simulate flashy hydrographs of the Doce River in Brazil after the failure of the Fundão Tailings Dam. This dam with a height of 120 m collapsed on November 5, 2015, and caused the propagation of a large flood along 550 km of the Doce River, until its final destination in the Atlantic Ocean (ANA 2016a). The observed hourly discharges at multiple stations on the Doce River provided an opportunity to test and revisit some of the most traditional flood routing procedures found in the literature, with potential development of an improved way to solve the Saint-Venant equations.

The main objectives of this paper are: (1) to analyze the features of widespread 1D flood routing methods; (2) to develop a new solution for the flood wave propagation problem using the diffusive wave format of the Saint-Venant equation; and (3) to compare these methods in a benchmark setting and to test with the observed hydrographs of the Doce River after the 2015 dam break.

Flood Routing Models

Overview of Models

Conservation of mass and momentum in a channel with variable cross section define the governing equations generally used to solve flood wave propagation in open channels. The 1D formulations as a function of distance x and time t are, respectively

$$\frac{\partial Q}{\partial x}+\frac{\partial A}{\partial t}=0 \tag{1}$$

$$\frac{\partial Q}{\partial t}+\frac{\partial}{\partial x}\left(\frac{Q^2}{A}\right)+gA\frac{\partial h}{\partial x}+gA(S_f-S_o)=0 \tag{2}$$

where Q = discharge, A = cross-section area, h = flow depth, S_o = river bed slope, S_f = slope of the energy grade line, and g = gravitational acceleration. These equations neglect minor contributions from the lateral inflow, wind shear and local losses due to abrupt contractions or expansions (Chow 1988). In addition, the main assumptions in the derivation of the Saint-Venant equations are (Akan 2006; Chaudhry 2007): (1) the velocity is uniformly distributed over the cross section; (2) the pressure is hydrostatic; (3) the fluid is homogeneous and incompressible; (4) the average channel bed slope is small; and (5) the resistance coefficients for steady uniform turbulent flow are applicable, and Manning's equation can be used to approximate the resistance to flow.

The terms of Eq. (2) describe the physical processes governing the flow momentum. Thus, the local acceleration term $\partial Q/\partial t$ describes the change in momentum over time, the convective acceleration term $(\partial/\partial x)(Q^2/A)$ denotes the change in momentum due to the downstream change in velocity along the channel, the pressure gradient term $gA(\partial h/\partial x)$ is proportional to the change in the water depth along the channel, the gravitational force term gAS_o is proportional to the bed slope S_o, and the friction force term gAS_f is proportional to the friction slope S_f. The application of the 1D momentum equation to a wide rectangular cross section results in the following simplified dimensionless form (Chow 1988; Sturm 2009; Julien 2018):

$$S_f \cong S_o-\frac{\partial h}{\partial x}-\frac{U}{g}\frac{\partial U}{\partial x}-\frac{1}{g}\frac{\partial U}{\partial t} \tag{3}$$

(I) (II) (III) (IV) (V)

Kinematic ⟷

Diffusive ⟷

Dynamic ⟷

Eq. (3) is useful in classifying different flood wave propagation models. The simplest model is the kinematic wave $(S_f=S_o)$, where the hydrograph is translated downstream without any peak discharge attenuation. The full dynamic wave equation is important when all acceleration terms [Terms IV and V of Eq. (3)] are relatively large when compared with the bed slope. This dynamic wave approximation is relevant for flood routing in mild slope rivers or fast rising hydrographs such as those from a breaching dam (USDA 2014). However, as stated by Ponce (2014), the dynamic wave is strongly diffusive (results in high peak discharge attenuation) especially for flows in the subcritical regime. Thus, in most rivers with subcritical flow, the flood wave propagation can be properly simulated by the diffusive wave approximation. This model corresponds to the case where the acceleration terms are negligible, thus the reduced momentum equation becomes

$$S_f \cong S_o-\frac{\partial h}{\partial x} \tag{4}$$

A criterion to check the applicability of the diffusive wave is given by Ponce (2014):

$$P=T_r S_o\left(\frac{g}{h_o}\right)^{0.5} \tag{5}$$

where T_r = hydrograph rising time (from low flow to peak) in seconds; and h_o = average flow depth in meters. The author suggested that the diffusive wave approximation is recommended when $P \geq 15$.

Classical Diffusive Wave Model

Eq. (4) can be converted into an advection-dispersion equation when coupled with the continuity and the resistance to flow given by the channel conveyance $(Q=K\sqrt{S_f})$. The derivation of this equation has been presented in different ways by several authors (Hayami 1951; Dooge and Harley 1967; Roberson et al. 1998; Chanson 2004; Sturm 2009; Szymkiewicz 2010; Battjes and Labeur 2017) and results in:

$$\frac{\partial Q}{\partial t}+C_e\frac{\partial Q}{\partial x}=D\frac{\partial^2 Q}{\partial x^2} \tag{6}$$

Eq. (6) is the linear diffusive wave model where C_e = flood wave celerity (flood wave propagation speed); and D = hydraulic diffusivity coefficient (flood wave attenuation factor), where both variables are treated as constants (Hayami 1951; Dooge and Harley 1967; Roberson et al. 1998). Here a distinction should be made

between the flood wave celerity C_e and the celerity $\sqrt{gh}$ of a small perturbation in a frictionless flow. The ratio between the flow velocity and this small perturbation defines the Froude number $Fr = U/\sqrt{gh}$.

One can write the discharge as a function of parameters (α and β) dependent on the resistance coefficient adopted (Manning, Darcy–Weisbach or Chézy)

$$Q = W\alpha h^{\beta} \tag{7}$$

where $\alpha = \sqrt{S_o}/n$; and n = Manning's coefficient in SI units. The flood wave celerity can be expressed as a function of the mean flow velocity U according to the Kleitz–Seddon relationship $C_e = \beta U$, where β gives the ratio between mean flow velocity and celerity, which can assume different values depending on the roughness coefficient (e.g., Manning, Darcy–Weisbach or Chézy) and the shape of the channel cross section (Julien 2018). For instance, considering Manning's relationship in a wide rectangular channel gives $\beta = 5/3$. Finally, the hydraulic diffusivity can be written as (Sturm 2009)

$$D = \frac{K^2}{2WQ} = \frac{K}{2W\sqrt{S_f}} \tag{8}$$

Considering $Q = K\sqrt{S_f}$ and the energy slope is equal to the bed channel slope, one can obtain the practical relationship for hydraulic diffusivity (Chaudhry 2007; Sturm 2009; Battjes and Labeur 2017)

$$D = \frac{Q_o}{2WS_o} \tag{9}$$

The assumption that the bed slope is equal to the energy slope in this last equation can be verified from Eq. (4) over a flood wave cycle in fluvial reaches neglecting backwater. One should see this during the rising limb of a hydrograph ($\partial h/dx < 0$) with the energy slope greater than the bed slope ($S_f > S_o$). The opposite is observed during the falling limb ($\partial h/dx > 0$ and $S_f < S_o$). Over a flood cycle, the average value of S_f is approximately equal to the bed slope S_o.

For the practical applications of the diffusive wave model the flood wave celerity can be obtained by iteration, considering the average value of flood wave celerity ($C_e = \beta U$) along the channel. However, it is not clear in the literature which reference discharge Q_o should be used to calculate D in Eq. (9). The mean and maximum discharges of the input hydrograph are natural choices. However, for a quick rising hydrograph from a dam break, the discharge can vary quickly both in time and space, and the use of peak discharge may lead to excessive diffusivity (excessive flood wave attenuation). Perhaps the flow discharge is not the best parameter to be used in the linear model.

The implementation of this flood routing model can be made through the FDM using numerical schemes such as the Crank Nicolson and QUICKEST, for instance (Szymkiewicz 2010). Eq. (9) is also implicitly contained in the Muskingum–Cunge method (Szymkiewicz 2010; Ponce 2014).

New Way to Solve the Diffusive Wave Model

Herein, a new way to solve the diffusive wave model is proposed, addressing two issues to improve the calculation of the quickly rising flow hydrographs in rivers: (1) define the diffusivity coefficient D in a way less dependent on a rapidly varied discharge as defined in the classical diffusive wave model [i.e., Eq. (9)], and (2) to include all terms of the Saint-Venant equation in this model.

Considering a wide rectangular channel it is possible to convert the terms in Eq. (3) into an equivalent form of Eq. (4) from $\partial h/\partial t = -\partial q/\partial x$. As shown by Julien (2018), one can reduce the full dynamic wave equation into an equivalent diffusive wave format as

$$S_f = S_o - [1 - (\beta - 1)^2 Fr^2]\frac{\partial h}{\partial x} \tag{10}$$

The term in brackets is the flood wave diffusivity $\Omega = [1 - (\beta - 1)^2 Fr^2]$, which depends on $\beta = C_e/U$ (the ratio between the flood wave celerity C_e and the mean flow velocity U) and the Froude number Fr. Hence, the full dynamic equation can be written in a similar format of the diffusive wave as

$$S_f = S_o - \Omega\frac{\partial h}{\partial x} \tag{11}$$

The inclusion of Ω takes into account the terms dropped in the derivation of the diffusive wave approximation. Accordingly, a similar procedure is used for the derivation of the diffusive wave approximation, and Eq. (6) simply becomes

$$\frac{\partial Q}{\partial t} + C_e\frac{\partial Q}{\partial x} = D_M\frac{\partial^2 Q}{\partial x^2} \tag{12}$$

where $D_M = \Omega D$. However, the remaining concern is the need to select a reference discharge for the calculation of the hydraulic diffusivity coefficient, which is a caveat of the linear diffusive wave routing procedure. The novel approach proposed here is to define the modified hydraulic diffusivity coefficient D_M as a function of the Froude number Fr and the flood wave celerity C_e, which are parameters with relatively small variances along a channel during a flood event. For the derivation of the modified diffusivity coefficient the conveyance K in a wide rectangular channel (i.e., $K = Q/\sqrt{S_o}$) is rewritten in the following form, considering the energy slope equal to the bed channel slope:

$$K = \frac{\alpha W}{\sqrt{S_o}}\left(\frac{U^2}{Fr^2 g}\right)^{\beta} \tag{13}$$

The substitution of Eq. (13) and $C_e = \beta U$ into $D_M = \Omega D$, considering $D = K/2W\sqrt{S_o}$ from Eq. (8) leads to

$$D_M = [1 - (\beta - 1)^2 Fr^2]\frac{\alpha}{2S_o}\left[\frac{1}{g}\left(\frac{C_e}{\beta Fr}\right)^2\right]^{\beta} \tag{14}$$

For Manning's equation in SI, the parameters of Eq. (14) are:

$$\alpha = \frac{\sqrt{S_o}}{n}, \qquad \beta = \frac{5}{3} \tag{15}$$

and, the modified diffusivity coefficient from Eqs. (14) and (15) becomes

$$D_M = \left[\frac{(1 - 0.444Fr^2)}{2n\sqrt{S_o}}\right]\left(\frac{0.6C_e}{Fr\sqrt{g}}\right)^{10/3} \tag{16}$$

There are two advantages to this formulation of the modified hydraulic diffusivity coefficient D_M: (1) it takes into account the full dynamic acceleration terms neglected in the derivation of the diffusive form; and (2) the reference discharge Q_o in the linear diffusive model [Eq. (9)] is replaced with parameters Fr and C_e, which remain fairly constant during floods (which is more coherent with the linear model assumption).

This new way to solve the diffusive model can be implemented using the same numerical schemes applied to the solution of the classical diffusive wave model (Crank Nicolson and QUICKEST). The main difference is the use of the modified coefficient D_M [Eq. (16)] instead of the traditional coefficient D [Eq. (9)].

This new approach will be tested and compared with other flood routing models in a benchmark test and in a real case of the flood wave propagation in the Doce River after the failure of the Fundão Dam in Brazil.

Numerical Solutions Procedures

Herein the classical diffusive wave model is solved using three different numerical schemes: Crank Nicolson, QUICKEST, and the Muskingum–Cunge method, all implemented in MATLAB version R2018b. These numerical schemes are also compared to the commonly used Preissmann scheme in HEC-RAS for the full dynamic wave model. Each scheme is briefly described below with more details in the Appendix.

Crank Nicolson Scheme

The Crank Nicolson (CN) scheme can be applied to solve advection-dispersion transport equations, which can represent different physical processes. In this article, this method is used to solve the classical and the new diffusive wave models, i.e., Eqs. (6) and (12), respectively. The accuracy of finite-difference schemes is introduced here; it describes how fast the approximation errors reduce to zero when Δx and Δt approach zero (Abbott and Basco 1990). Thus, the Crank Nicolson scheme is second-order accurate (faster reduction of truncation error than first-order schemes). Furthermore, this scheme is unconditionally stable and does not cause numerical dissipation, even though it can present phase errors and result in oscillations if large time steps are chosen (Moin 2010; Szymkiewicz 2010).

QUICKEST Scheme

The QUICKEST (Quadratic Upstream Interpolation for Convective Kinematics with Estimated Streaming Terms) is an explicit scheme developed by Leonard (1979). This is a third-order scheme to solve unsteady flows in the format of advection-dispersion, i.e., the diffusive wave model [Eqs. (6) or (12)]. The method does not present numerical dissipation; however, due its explicit nature, the stability is conditioned on the choice of the mesh size (Leonard 1979; Szymkiewicz 2010; Julien 2018).

Muskingum–Cunge Method

The Muskingum–Cunge (MC) method is a modification of the Muskingum method where the diffusive wave approximation is applied instead of the kinematic wave. In general, the wide rectangular channel assumption is implicit in its derivation. It also considers the hydraulic diffusivity from Eq. (9). The accuracy can deteriorate in mild slope rivers (Price 2009).

Preissmann Scheme

The Preissmann scheme is arguably the most popular method extensively used in commercial codes (Zijlema 2015; Battjes and Labeur 2017). It is accepted as a robust scheme for being stable without time-steps limitations (Szymkiewicz 2010; Rowinski and Radecki-Pawlik 2015). However, this method can result in nonphysical smoothing, which becomes significant when strong gradients occur in the solution (Szymkiewicz 2010).

This scheme considers weight coefficients for the time derivative ψ and for the space derivative θ. The time derivative is generally computed with $\psi = 0.5$ (Abbott and Basco 1990), and the scheme is unconditionally stable, but displays numerical dissipation when $0.5 < \theta \leq 1$. For practical applications, the parameter θ usually ranges from 0.6 to 1; the value of $\theta = 0.6$ results in more accurate solutions, but it is more susceptible to instabilities. Conversely, the value of $\theta = 1.0$ (the fully implicit scheme) provides the most stable solutions (USACE 2016d). For many real-world simulations, there are no significant differences in the results when changing θ from 1.0 to 0.6 (USACE 2016d). More details about this method can be easily found in the literature or in software manuals (Akan 2006; Wu 2007; Sturm 2009; Szymkiewicz 2010; USACE 2016d).

The Preissmann scheme is a first-order method, which means that approximation errors slowly approach zero, when compared with second- and third-order schemes. This scheme is readily available in HEC-RAS, herein using the version 5.0.1 (USACE 2016d). HEC-RAS is a very popular software and is one of the 1D models recommended for downstream routing of the breach hydrograph in the US according to federal guidelines for inundation mapping of flood risk associated with dam incidents and failures (FEMA 2013).

A summary of the main features of each method is given on Table 1.

Table 1. Summary of characteristics of widespread methods to calculate flood routing

Numerical approach	Continuity equation	Full dynamic wave equation	Diffusive wave equation	Accuracy order	Comments
Crank Nicolson	—	—	X	2nd	Implicit, nondiffusive and unconditionally stable. It can be dispersive (oscillations of the solution) depending on the mesh size. The hydraulic diffusivity coefficient must be known in advance and requires an additional method or function to calculate the water level
QUICKEST	—	—	X	3rd	Explicit and nondiffusive. Its stability is defined by a stability diagram depending on the choice of the Courant numbers (C_a, C_d). The hydraulic diffusivity coefficient must be known in advance and requires an additional method or function to calculate the water level
Preissmann	X	X	—	1st	Implicit, unconditionally stable and presents numerical dissipation when $0.5 < \theta \leq 1$. Can result in unphysical smoothing when sharp gradients occur on the solution. It is available in HEC-RAS
Muskingum–Cunge	X	—	X	1st	Explicit, unconditionally stable. It loses accuracy as the river bed slope becomes milder. Requires an additional method or function to calculate the water level

Test Setup Description

Two tests are proposed to compare the performance of the presented models: (1) a hypothetical channel under a range of bed slopes and time-to-peak of the input hydrograph; and (2) a real case of the flood wave propagation in the Doce River after the collapse of the Fundão Dam in Brazil. The tests are described in the following sections.

Benchmark Testing for a Hypothetical Channel

To compare the performance of the flood routing models considering a wide range of parameters (bed slope and time to peak), the simulation of a hypothetical channel is first considered. This is a 50 km-long channel, with a width of 100 m (wide rectangular) and Manning n equal to 0.03. Three different slopes are considered: 0.01, 0.001, and 0.0001. One should note that steep slope channels are not the focus of this paper; however, it is only used in the benchmark testing for comparison of the effect of the bed slope on the flood routing models.

As an upstream boundary condition, a flashy hydrograph with similar features to the Fundão Dam collapse in the Doce River is simplified as a triangular hydrograph, varying from 30 to 2,000 m^3/s. To test the effect of the flashiness, two different rising times T_r were considered (3h and 15 h), providing a wide range of Ponce parameter P (from 1 to 1,211) when considering three bed slopes. The flood routing models tested are: (1) the classical diffusive wave model using the Crank Nicolson, QUICKEST scheme, and Muskingum–Cunge, (2) the dynamic wave model using the Preissmann scheme, and (3) the new diffusive wave model using the Crank Nicolson and QUICKEST scheme.

The HEC-RAS reference manual (USACE 2016d) provides a starting point for the estimation of the cross-section distance Δx in dam break simulations. Accordingly, it can be determined by the following expression:

$$\Delta x \leq \frac{0.15H}{S_o} \tag{17}$$

where Δx = distance between the cross-sections in meters; and H = average main channel bankfull depth in meters. An alternative equation for Δx is

$$\Delta x \leq \frac{C_e T_r}{20} \tag{18}$$

where C_e = celerity (wave speed) in m/s; and T_r = hydrograph rising time in seconds. An initial guess for the wave celerity can be done using by the Kleitz–Seddon equation (Chanson 2004; Julien 2018)

$$C_e = \frac{\partial Q}{\partial A} \approx \frac{\Delta Q}{\Delta A} \tag{19}$$

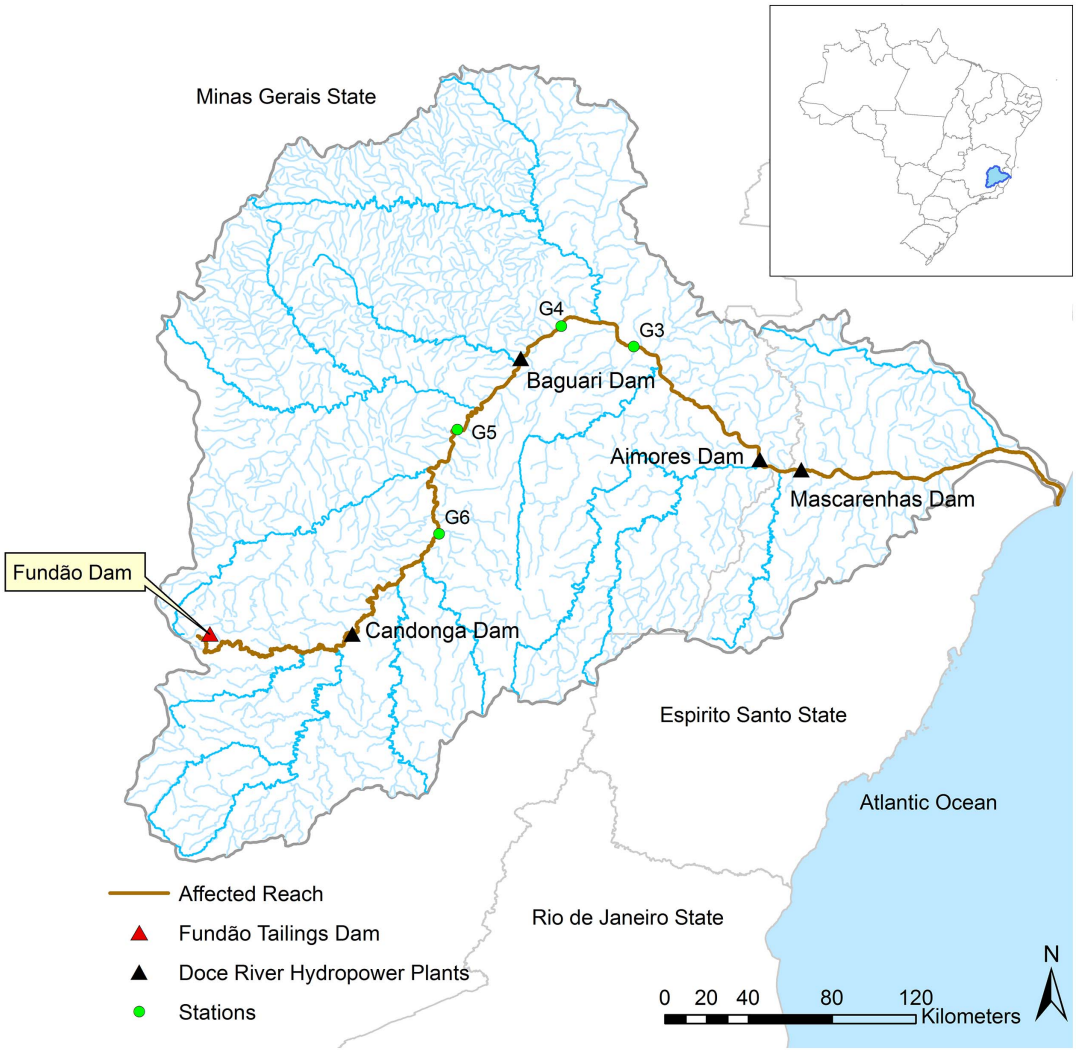

Fig. 1. Doce River basin: location of the Fundão Dam and the gaging stations.

Furthermore, a practical time step Δt for medium to large rivers is given by USACE (2016d)

$$\Delta t \leq \frac{T_r}{20} \tag{20}$$

The expressions above are useful in setting up the initial mesh size for the benchmark test.

Fundão Dam Failure Case

The Fundão Dam was located in the upper Doce River basin, in the southeast region of Brazil, as shown in Fig. 1. This basin has a drainage area of 82,600 km^2 and the Doce River extends 550 km to the Atlantic Ocean. The Fundão Dam collapsed on November 5, 2015, around 16:00 h (Morgenstern et al. 2016). Then the flood of the Doce River started on November 6 (CPRM and ANA 2015; Palu and Julien 2019), and reached the Atlantic Ocean on November 11 (Palu 2019).

The propagation of the flood wave in the Doce River was registered at four stations of the alert system of critical events of the geological survey of Brazil and the National Water Agency, designed to alert the towns around the Doce River about flood risks during the rainy season (CPRM and ANA 2016). Table 2 presents the description of the stations and the type of data available.

The flood propagated only in the main channel of the Doce River, not reaching the floodplain. Fig. 2 shows the resultant flashy hydrographs registered by stations along the Doce River. Despite the distance from the dam collapse, the observed hydrograph rose quickly when compared with natural floods. For instance, at the first hydropower reservoir (Candonga Dam) the hydrograph rising time was 3 h (from 30 to 2,000 m^3/s), at gaging station G6 it was 8.5 h (60 to 900 m^3/s), 9 h for station G5 (75 to 700 m^3/s), and approximately 9.5 h for station G4 (100 to 630 m^3/s). This rising time of natural floods is about 140 h (Table 3). In order to quantify the hydrograph flashiness (rate of change in flow) after the dam break, the Richards–Baker flashiness index is considered (Baker et al. 2004):

$$R - B \text{ Index} = \frac{\sum_{i=1}^{N} |Q_i - Q_{i-1}|}{\sum_{i=1}^{N} Q_i} \tag{21}$$

where Q_i refers to discharge for a time i and N is the number of observations. For comparison, the index is also applied to a natural flood event in the Doce River between December 2016 and January 2017 which lasted for approximately 30 days according to data from the National Water Agency (ANA 2017). Table 3 shows the results considering hourly discharge measurements. As one can observe, the flashiness index for the hydrograph after the dam break is upto 15 times higher than for natural floods in the same river.

The test of the flood routing models focuses on two fluvial reaches (Reaches 1 and 2) for which high-quality discharge measurements were available on an hourly basis. Reach 1 is located between the stations G6 and G5 and extends 74 km at an average width of 200 m. The second reach (Reach 2) is 60 km long located between the stations G5 and G4, with an average width of 280 m. The cross sections at stations G6 and G4 are presented in Fig. 3.

The bed slope for both reaches is equal to 0.0005, obtained from the digital elevation model of the Doce River basin at a spatial resolution of 10 m, provided by the National Water Agency (Geonetwork 2007). Daily mean water level data from the reservoir monitoring system of the National Water Agency (ANA 2016b) showed negligible flood peak attenuation in the Baguari Reservoir (between stations G5 and G4).

Table 2. Available data on the Doce River's gaging stations

ID	Station name	Type	NWA code	Data available
G6	Cachoeira dos Óculos	Telemetric	56539000	Discharge each 15 min, cross-section and stage-discharge curve
G5	Belo Oriente	Telemetric	56719998	Discharge each 15 min, cross-section and stage-discharge curve
G4	Governador Valadares	Telemetric	56850000	Discharge each 1 h, cross-section and stage-discharge curve
G3	Tumiritinga	Conventional	56920000	Discharge with two measurements per day, cross-section and stage-discharge curve

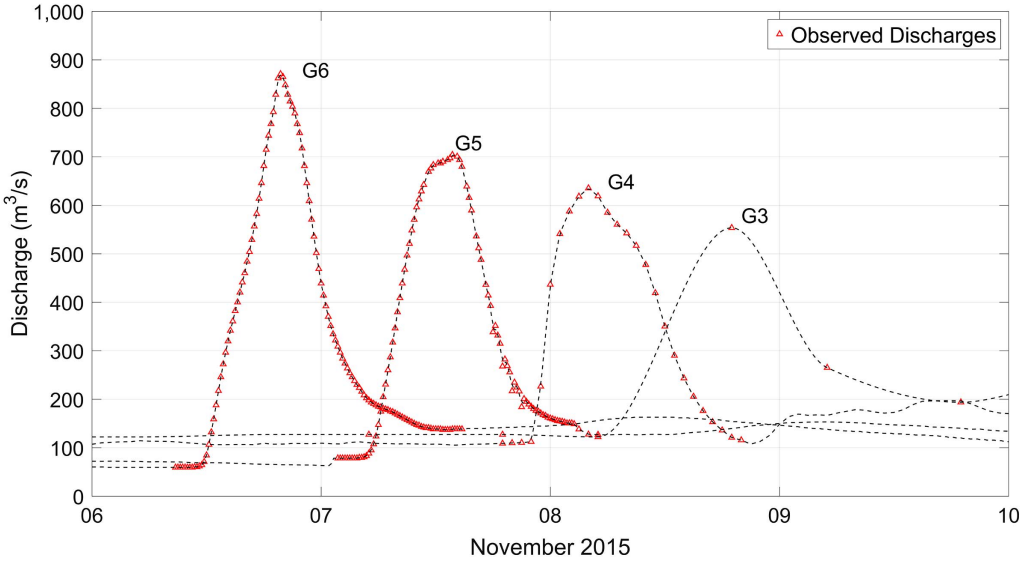

Fig. 2. Observed hydrographs in the Doce River after the Fundão Dam collapse. (Data from ANA 2017.)

Table 3. Analysis of hydrograph flashiness

Station	Fundão Dam break Tr(h)	P	Flashiness index	Natural flood (2016–2017) Tr(h)	P	Flashiness index
G6	8.5	21	0.17	144	345	0.011
G5	9.0	29	0.14	139	378	0.011
G4	9.5	35	0.11	146	371	0.019

Note: Based on hourly measurements.

Flood Routing Results

Benchmark Testing Results

Initially, the hypothetical channel with the mild slope $S_o = 0.0001$ considering $T_r = 3$ h was used in the analysis of the mesh, since it was the closest combination to simulate the flood wave propagation after a dam break in a natural stream. Fig. 4 shows the results of analysis of mesh size for the different methods. The left-hand side

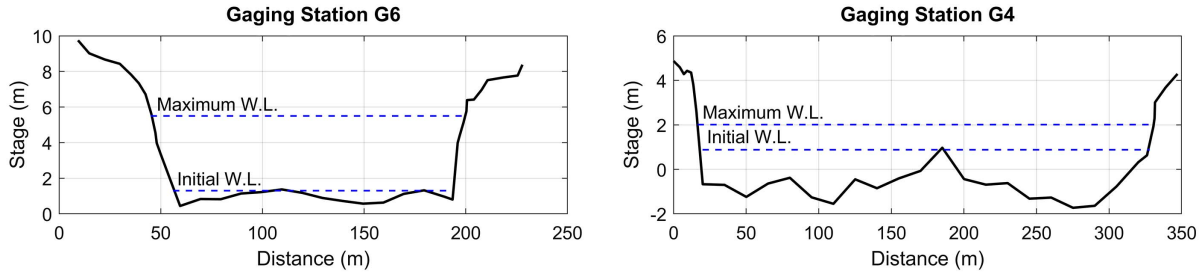

Fig. 3. Doce River cross sections at stations G6 and G4.

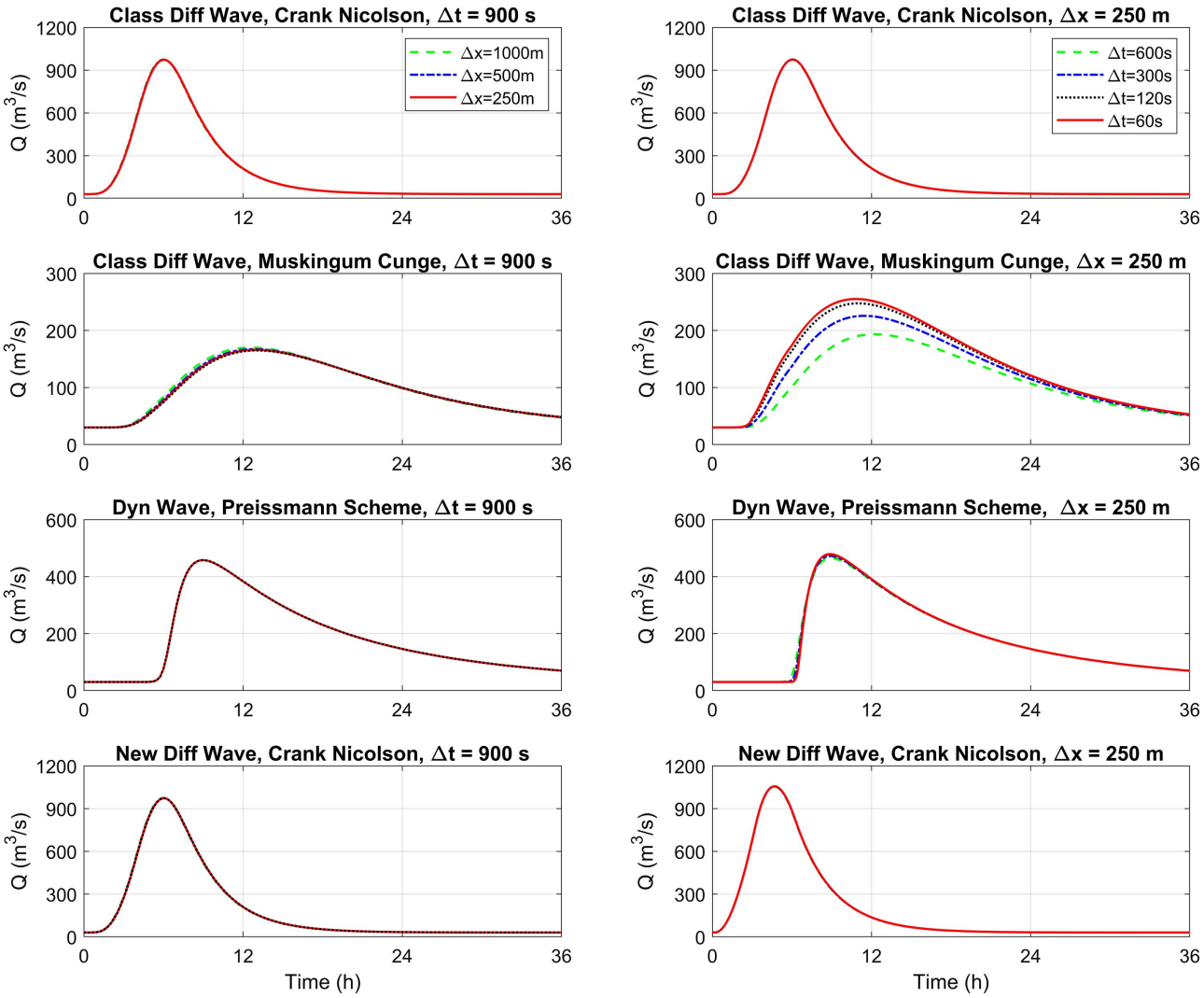

Fig. 4. Mesh analysis for the flood routing simulation for different methods.

of Fig. 4 shows the effect of varying Δx while $\Delta t = 900$ s, and the right-hand side shows the effect of varying Δt while $\Delta x = 250$ m. The final mesh size selected for all schemes was $\Delta x = 250$ m and $\Delta t = 60$ s, since no substantial improvements were observed with more refinements, even though it was clear that the models presented different degrees of flood wave attenuation. For the diffusive wave models there was no noticeable difference between the Crank Nicolson and QUICKEST scheme; for this reason only the Crank Nicolson scheme is presented. After the mesh analysis, the attenuation of the peak discharge for each model is presented in Fig. 5.

During the simulations the dynamic wave model using the Preissmann scheme and the classic diffusive wave model using Muskingum–Cunge presented oscillations in the steepest channel ($S_o = 0.01$). Despite this, all other models presented similar attenuation of the flood wave. On a mild bed slope ($S_o = 0.001$), the simulation of flashy hydrographs ($T_r = 3$ h) showed some divergence in the results. One can observe that at the same slope, the results for the slower peak ($T_r = 15$ h) are very similar for all models. Finally, the test of the mildest channel ($S_o = 0.0001$) with the flashiest hydrograph ($T_r = 3$ h) presented the largest divergence among the models. The classic diffusive model solved using the Muskingum–Cunge model presented the maximum diffusivity ($Q/Q_{\max} = 0.13$); conversely, the new way to solve the diffusive wave model using the Crank Nicolson scheme resulted in the most conservative peak discharge attenuation ($Q/Q_{\max} = 0.57$). Contrary to expectation, this last simulation ($S_o = 0.0001$ and $T_r = 3$ h) resulted in a larger attenuation at a low Ponce parameter ($P = 1$) for the dynamic wave model rather than for the diffusive wave model. Even though the dynamic wave model considers all terms of the momentum equation, the excessive diffusivity of the flood wave can be attributed to the combination of the strong flood wave diffusivity implicit in the dynamic wave model (Ponce 2014) with the numerical dissipation of the Preissmann scheme,

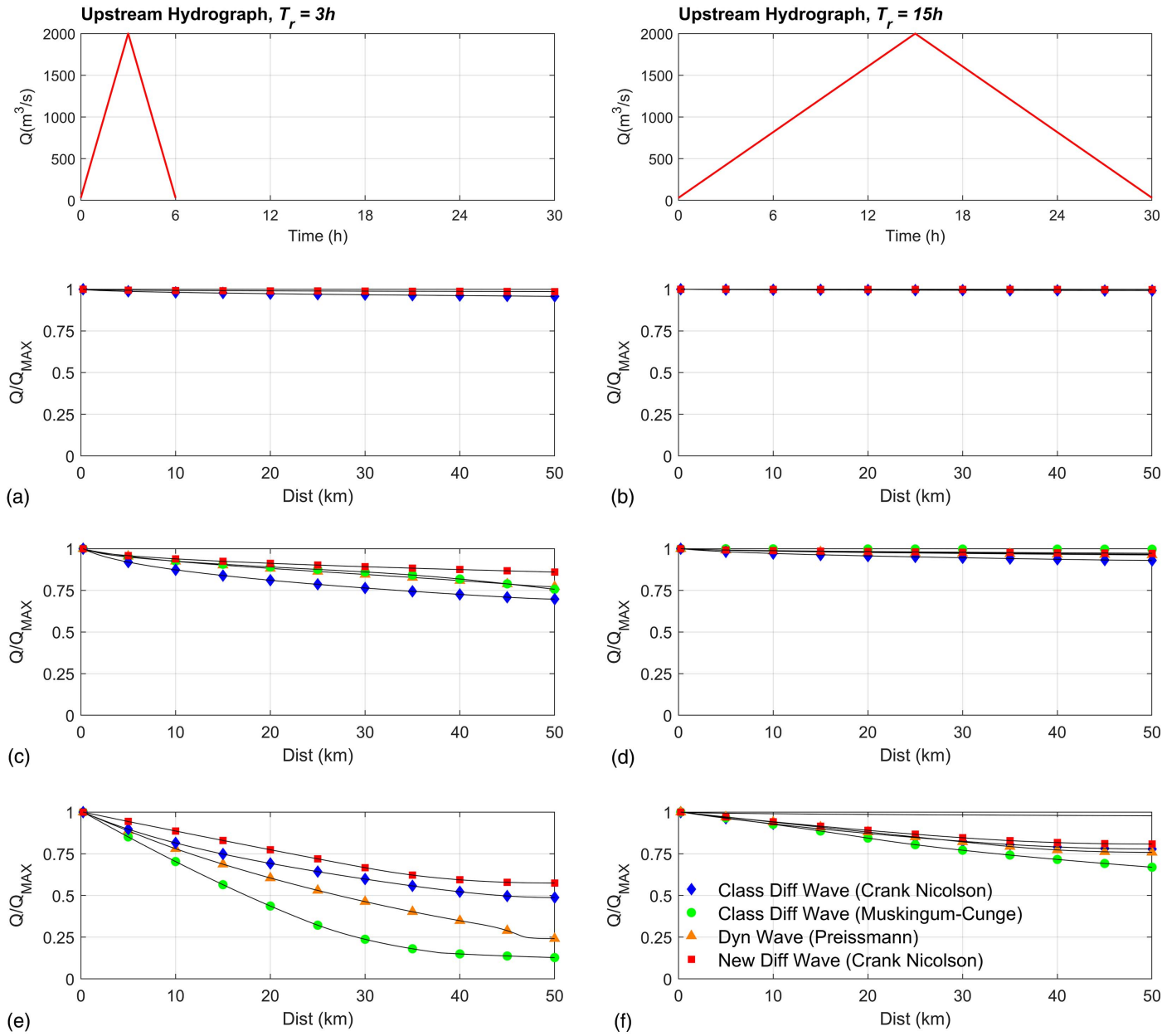

Fig. 5. Comparison of the flood wave attenuation in a hypothetical channel for different methods: (a) $S_o = 0.01$, $P = 242$; (b) $S_o = 0.01$, $P = 1211$; (c) $S_o = 0.001$, $P = 17$; (d) $S_o = 0.001$, $P = 86$; (e) $S_o = 0.0001$, $P = 1$; and (f) $S_o = 0.0001$, $P = 6$.

J. Hydraul. Eng., 2020, 146(6): 04020043

which is magnified for sharp hydrographs. In contrast, these same effects were not observed for the diffusive wave models solved using the Crank Nicolson and QUICKEST scheme. Both schemes do not present numerical dissipation; moreover, we note that the new way to solve the diffusive wave presented more conservative results in terms of flood wave attenuation when compared with other tested models. Now the next step is to test these algorithms on the Doce River after the Fundão Dam collapse.

Fundão Dam Case Results

The flood routing models were tested for flood wave propagation in two Doce River reaches after the Fundão Dam collapse. The calibration of the models was based on historical stage-discharge data of the National Water Agency collected at stations G6, G5, and G3 (ANA 2017), since these stations presented better-quality measurements. The estimated Manning's n roughness coefficient at each station are 0.056, 0.046, and 0.047, respectively (Palu 2019). Thus, an average Manning's coefficient equal to 0.05 for the first reach (between stations G6 and G5) and 0.047 for the second reach (between stations G5 and G4) was used for all flood routing models. These values present an estimate of the natural roughness of the river, and the use of these coefficients resulted in proper flood wave celerity. A sensitivity analysis carried out showed that the application of smaller roughness accelerated the hydrograph and higher values resulted in delayed propagation. The initial condition for all models was the initial observed discharge starting from the steady state (60 m^3/s for Reach 1 and 75 m^3/s for Reach 2). The upstream boundary condition was the observed hydrographs at stations G6 and G5 while the downstream hydraulic boundary condition was the normal depth consideration. The mesh analysis resulted in the same values as the benchmark testing ($\Delta x = 250$ m and $\Delta t = 60$ s).

A summary of the simulation parameters is presented on Table 4, while Figs. 6 and 7 show the result of the simulation in comparison with the observed hydrographs for Reaches 1 and 2, respectively. The quantitative comparison between the observed discharges and the numerical simulations is made using the relative percent difference (RPD) applied on the peak discharge, the root mean square error (RMSE), the mean absolute percentage error (MAPE), and the difference in the time of peak, as presented in Table 5.

Table 4. Summary of parameters for the flood routing simulations using different models

Parameter	Reach 1 (G6 to G5)	Reach 2 (G5 to G4)
L (km)	74	60
W (m)	200	280
S (m/m)	0.0005	0.0005
Manning n	0.05	0.047
H (m)	6.5	5.6
Tr (h)	8.5	9.5
Δx min (m)	2,050	1,080
Δx adopted (m)	250	250
Δt minimum(s)	1,670	1,530
Δt (s) adopted	60	60
Fr	0.19	0.18
θ (Preissmann scheme)	1.0	1.0
	Diffusive wave model	
P (Ponce parameter)	26	38
C_e (m/s) initial guess	1.34	1.0
C_e (m/s) final	1.19	1.04
Q_{ref} (m^3/s)	465	384
D (m^2/s)	2,325	1,370
	New dynamic wave model	
Ω	0.98	0.99
D_M (m^2/s)	740	663

In terms of flood attenuation, the results were coherent with the benchmark testing. For the case of the classic diffusive wave models solved with the Crank Nicolson and QUICKEST schemes, the issue concerned the determination of the hydraulic diffusivity coefficient, which was overestimated by the expression from the literature [Eq. (9)]. The result was an excessively diffused hydrograph with both methods, with the peak underestimated by 18%. The uncertainty about the reference discharge prevailed, since the mean discharge resulted in a poor estimation of D, while the use of the peak discharge would have led to even worse results (since it would have resulted in a higher D). The Muskingum–Cunge method presented low peaks, underestimating the peak discharge by 16%. For the Preissmann scheme the variation on the weight parameter θ from 0.6 to 1 did not result in any improvement. Moreover, it smoothed the solution by lowering the peak by 14%, when compared with the observed discharges. As observed in benchmark testing, the combination of a mild slope of the sharp hydrograph resulted in high flood wave diffusivity for this method. Ultimately, none of the classical methodologies tested presented a satisfactory fit with the observed data.

The application of the new way to solve the diffusive wave model, Eq. (16) on the Doce River was made using constant values of the Froude number and $\beta = 5/3$ (where β is not a calibration parameter). The roughness coefficient was the same calibrated for the classical models ($n = 0.05$ for the first reach, between stations G6 and G5 and $n = 0.047$ for the second reach, between stations G5 and G4).

The results considering the two numerical schemes (Crank Nicolson and QUICKEST) using the new approach are almost identical. For the QUICKEST scheme, for instance, the maximum reduction found was RPD (−18% to −0.1%), RMSE (72–34 m^3/s), and MAPE (32%–15%). The maximum difference found in the time of peak was about 1.2 h. Moreover, the results in both reaches are consistent, better fitting the observed data when compared with all the previous methodologies. In addition, the results obtained along the Doce River are also consistent with those from the hypothetical channel.

The enhanced performance of the new approach is mainly attributed to the modified hydraulic coefficient used on the linear model, which uses parameters with less variability (Froude number and celerity) rather than a highly variable discharge. It also takes into account the additional acceleration terms of the Saint-Venant equation in the full dynamic wave. Moreover, the numerical schemes used to integrate the Saint-Venant equations (Crank Nicolson and QUICKEST) are nondiffusive schemes, avoiding numerical dissipation.

Discussion and Conclusion

The applicability of different flood routing models to flashy hydrographs was tested on a hypothetical channel and in two Doce River reaches after the Fundão Dam failure. Classic models such as the diffusive wave model numerically solved using the Crank Nicolson, QUICKEST, and Muskingum–Cunge methods and the dynamic wave model solved using the Preissmann scheme produced excessive flood wave attenuation in a mild slope channel with a flashy hydrograph. Application of those methods in the real case of the Fundão Dam failure in Brazil resulted in unsatisfactory results; the peak discharge of the predicted hydrograph presented an error up to −18% when compared with measured hydrographs.

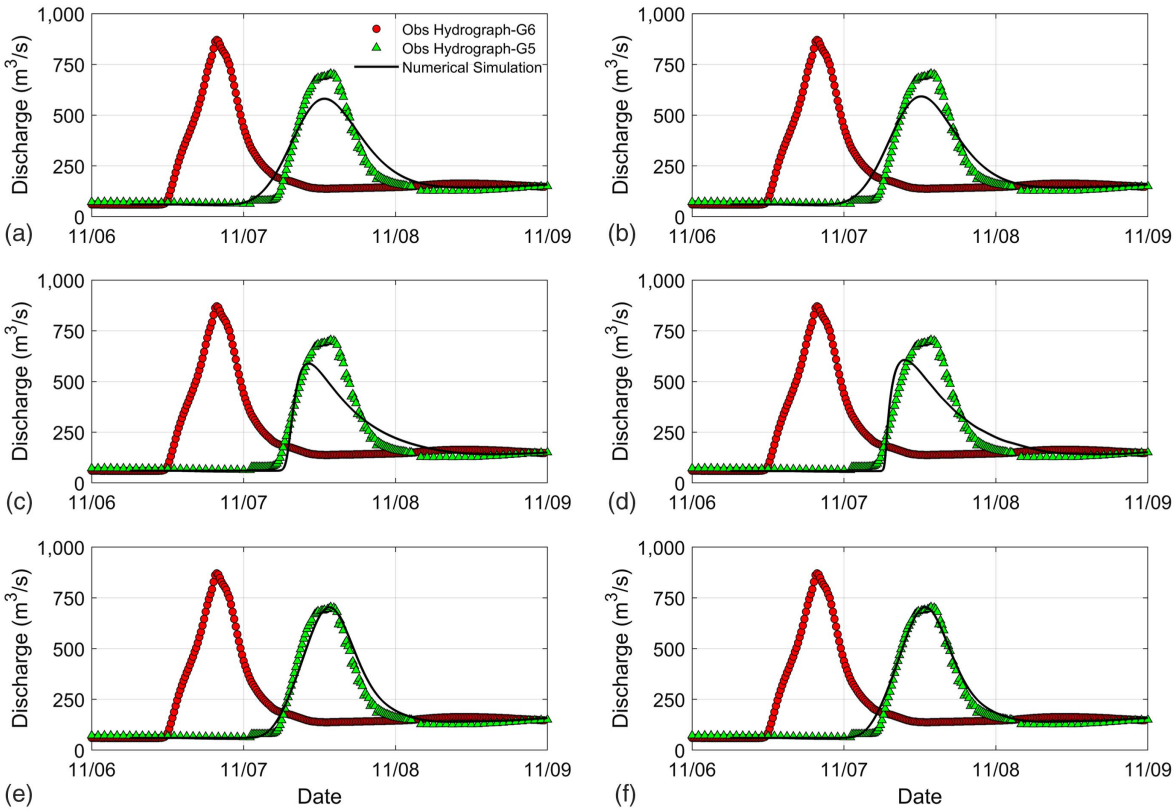

Fig. 6. Evaluation of flood routing methods in the Doce River, Reach 1: (a) classic diffusive wave—Crank Nicolson; (b) classic diffusive wave—QUICKEST; (c) classic diffusive wave—Muskingum–Cunge; (d) dynamic wave—Preissmann; (e) new diffusive wave—Crank Nicolson; (f) new diffusive wave—QUICKEST.

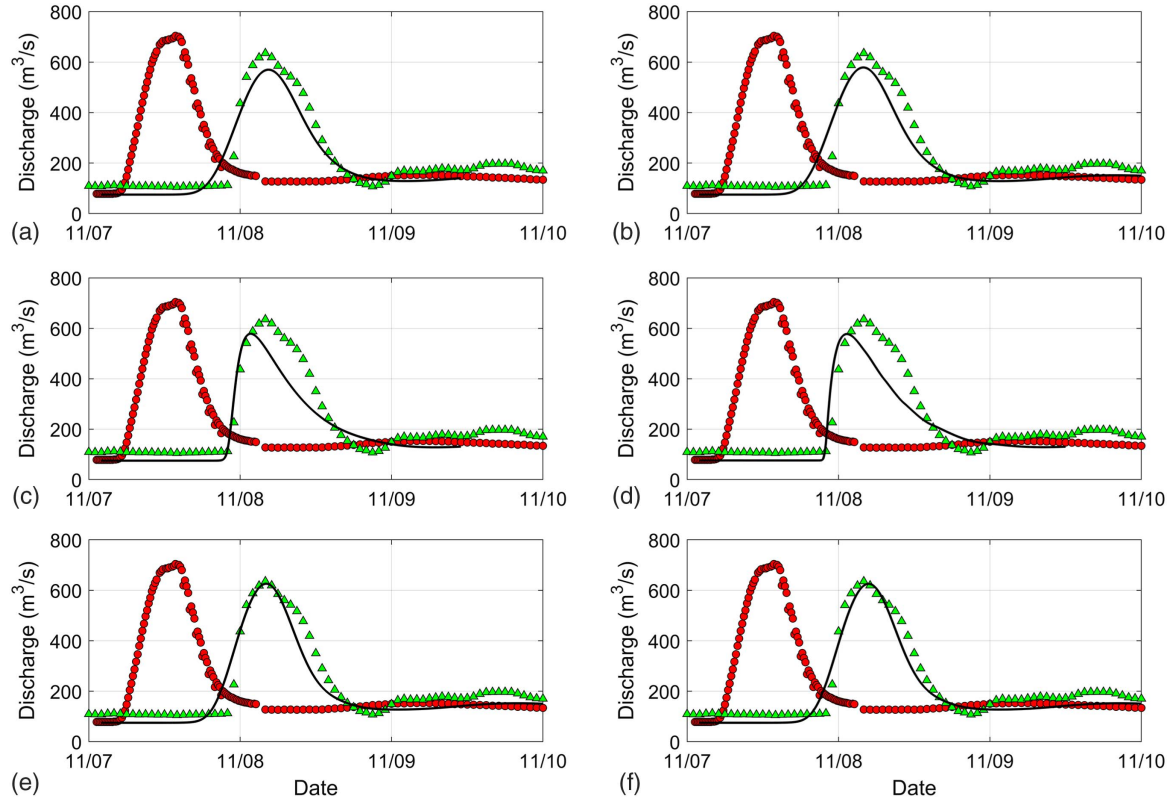

Fig. 7. Evaluation of flood routing methods in the Doce River, Reach 2: (a) classic diffusive wave—Crank Nicolson; (b) classic diffusive wave—QUICKEST; (c) classic diffusive wave—Muskingum–Cunge; (d) dynamic wave—Preissmann; (e) new diffusive wave—Crank Nicolson; (f) new diffusive wave—QUICKEST.

Table 5. Comparison between the observed hydrograph and the numerical simulations

		Reach 1					Reach 2				
Simulation	Method	Peak (m^3/s)	RPD (%)	RMSE (m^3/s)	MAPE (%)	Peak time Difference (h)	Peak (m^3/s)	RPD (%)	RMSE (m^3/s)	MAPE (%)	Peak time Difference (h)
—	Observed	704	—	—	—	—	635	—	—	—	—
A	Diffusive wave—Crank Nicolson	581	−18	72	30	−1.2	570	−10	58	31	0.83
B	Diffusive wave—QUICKEST	592	−16	72	32	−1.7	579	−9	68	33	0.17
C	Diffusive wave—Muskingum–Cunge	589	−16	84	23	−3.5	578	−9	78	23	−1.83
D	Dynamic wave—Preissmann	606	−14	89	25	−4.0	577	−9	85	24	−2.00
E	New diffusive wave—Crank Nicolson	704	−0.1	49	17	−0.4	626	−2	48	18	1.17
F	New diffusive wave—QUICKEST	704	−0.1	34	15	−1.2	626	−2	61	21	0.42

Efforts to refine the mesh, to calibrate the models, and to change scheme parameters, as Preissmann weight parameters θ for instance, did not improve the results.

A new way to solve the diffusive wave model was developed using the modified hydraulic diffusivity coefficient D_M, which considers all terms of the Saint-Venant equation. The coefficient D_M is a function of the Froude number Fr and flood wave celerity C_e, two parameters with relatively small variation along the channel during a flood event. The use of these parameters in Eq. (16) is more coherent with the linear model assumption and results in more realistic flood wave attenuation. The numerical solution could be implemented using the QUICKEST (explicit) or the Crank Nicolson (implicit) scheme, since both give very similar results without numerical dissipation.

The test of the methodology on a hypothetical channel and in two Doce River examples showed more conservative results in terms of flood wave attenuation and greatly improved the accuracy of the hydrograph predictions. It is a matter of preference whether the user wants to apply a simpler explicit subject to a conditioned mesh choice and proper handling of boundary conditions (QUICKEST), or an implicit scheme which is more flexible about the mesh size but requires greater computational effort (Crank Nicolson). These two schemes presented very similar results. For instance, the QUICKEST scheme decreased the error from −18% to −0.1% for RPD, 72 to 34 m^3/s for RMSE, and 32% to 15% for MAPE. The maximum difference found in the time of peak decreased from 5 to 1.2 h.

Appendix. Numerical Schemes for Flood Routing Calculation

Crank Nicolson

This scheme is given by the application of a central difference in space and the trapezoidal method for time advance in the diffusive wave approximation [Eq. (6)]

$$Q_{j+1}^{n+1}\left(\frac{C_a}{4}-\frac{C_d}{2}\right)+Q_j^{n+1}(1+C_d)-Q_{j-1}^{n+1}\left(\frac{C_a}{4}+\frac{C_d}{2}\right)$$
$$=-Q_{j+1}^{n}\left(\frac{C_a}{4}-\frac{C_d}{2}\right)+Q_j^{n}(1-C_d)+Q_{j-1}^{n}\left(\frac{C_a}{4}+\frac{C_d}{2}\right) \quad (22)$$

where Q_j^n refers to the discharge at the cross section j and in the time level n in the computational grid. In addition, C_a = the Courant number; and C_d = the diffusive Courant number, given by

$$C_a = C_e\frac{\Delta t}{\Delta x}$$
$$C_d = D\frac{\Delta t}{\Delta x^2} \quad (23)$$

The calculation of the discharges for the next time steps is made by matrix inversion. Once the discharges are calculated, the flow depth can be obtained by the discretization of the continuity equation. For instance, the leap-frog scheme (Mahmood and Yevjevich 1975) can be applied, since it is a second-order method:

$$h_j^{n+1}=h_j^{n-1}-\frac{\Delta t}{W\Delta x}(Q_{j+1}^n-Q_{j-1}^n) \quad (24)$$

QUICKEST Scheme

This scheme is given by Julien (2018)

$$Q_j^{n+1}=Q_j^n+\phi_1 Q_{j+1}^n-\phi_2 Q_j^n+\phi_3 Q_{j-1}^n+\phi_4 Q_{j-2}^n \quad (25)$$

where

$$\phi_1=C_d(1-C_a)-\frac{C_a}{6}(C_a^2-3C_a+2) \quad (26)$$

$$\phi_2=C_d(2-3C_a)-\frac{C_a}{2}(C_a^2-2C_a-1) \quad (27)$$

$$\phi_3=C_d(1-3C_a)-\frac{C_a}{2}(C_a^2-C_a-2) \quad (28)$$

$$\phi_4=C_d(C_a)+\frac{C_a}{6}(C_a^2-1) \quad (29)$$

Preissmann Scheme

The application of the Preissmann scheme for the Saint-Venant equations results in the discretized continuity and momentum equations

$$\frac{1}{W_p}\left[(1-\theta)\frac{Q_{j+1}^n-Q_j^n}{\Delta x}+\theta\frac{Q_{j+1}^{n+1}-Q_j^{n+1}}{\Delta x}\right]$$
$$+\psi\left(\frac{h_j^{n+1}-h_j^n}{\Delta t}+\frac{h_{j+1}^{n+1}-h_{j+1}^n}{\Delta t}\right)=0 \quad (30)$$

$$\psi\left(\frac{Q_j^{n+1}-Q_j^n}{\Delta t}+\frac{Q_{j+1}^{n+1}-Q_{j+1}^n}{\Delta t}\right)+\frac{(1-\theta)}{\Delta x}\left[\left(\frac{Q^2}{A}\right)_{j+1}^n-\left(\frac{Q^2}{A}\right)_j^n\right]$$
$$+\frac{\theta}{\Delta x}\left[\left(\frac{Q^2}{A}\right)_{j+1}^{n+1}-\left(\frac{Q^2}{A}\right)_j^{n+1}\right]$$
$$+gA_p\left[(1-\theta)\frac{h_{j+1}^n-h_j^n}{\Delta x}+\theta\frac{h_{j+1}^{n+1}-h_j^{n+1}}{\Delta x}\right]$$
$$+\left(\frac{gn_M^2|Q|Q}{R^{4/3}A}\right)_p-gA_pS_o=0 \quad (31)$$

where n and j are indexes of time level and cross section, respectively. The index P means that the function or expression

requires discretization. In addition, ψ and θ are weighting parameters varying from 0.5 to 1.

Muskingum–Cunge

This method is well described by Szymkiewicz (2010)

$$Q_j^{n+1} = C_1 Q_{j-1}^n + C_2 Q_j^n + C_3 Q_{j-1}^{n+1} \tag{32}$$

The coefficients C_1, C_2, and C_3 are equal to

$$C_1 = \frac{KX + 0.5\Delta t}{K(1-X) + 0.5\Delta t} \tag{33}$$

$$C_2 = \frac{K(1-X) - 0.5\Delta t}{K(1-X) + 0.5\Delta t} \tag{34}$$

$$C_3 = \frac{-KX + 0.5\Delta t}{K(1-X) + 0.5\Delta t} \tag{35}$$

where the parameters K and X are defined as

$$K = \frac{\Delta x}{Ce} \tag{36}$$

$$X = 0.5 - \frac{Q}{2\mathrm{WS}_o K C_e^2} \tag{37}$$

The parameters can be kept constant to a chosen reference discharge (linear approach), or updated using the known discharges at every time step (nonlinear) (Akan 2006; McCuen 2016).

Data Availability Statement

The data (discharge measurements) and codes generated in MATLAB during the study are available from the corresponding author by request.

Acknowledgments

The authors would like to acknowledge that this work was developed with the support of CNPq (Brazilian National Council for Scientific and Technological Development).

References

Abbott, M. B., and D. R. Basco. 1990. *Computational fluid dynamics: An introduction for engineers*. New York: Longman Sc & Tech.

Akan, A. O. 2006. *Open channel hydraulics*. Burlington, NJ: Butterworth-Heinemann.

ANA (Agência Nacional de Águas). 2016a. "Encarte especial sobre a bacia do Rio Doce–Rompimento da barragem em Mariana/MG." In *Conjuntura dos Recursos Hidricos no Brasil–Informe 2015*, 50. Brasilia-DF, Brazil: ANA.

ANA (Agência Nacional de Águas). 2016b. "SAR–Sistema de acompanhamento de reservatórios." Accessed April 12, 2016. http://sar.ana.gov.br/.

ANA (Agência Nacional de Águas). 2017. "HidroWeb." Accessed June 23, 2017. http://hidroweb.ana.gov.br/default.asp.

ANSYS (Analysis System). 2019. "ANSYS FLUENT 12.0 User's guide." Accessed March 25, 2019. http://www.afs.enea.it/project/neptunius/docs/fluent/html/ug/main_pre.htm.

Baker, D. B., R. P. Richards, T. T. Loftus, and J. W. Kramer. 2004. "A new flashiness index: Characteristics and applications to Midwestern rivers and streams." *J. Am. Water Resour. Assoc.* 40 (2): 503–522. https://doi.org/10.1111/j.1752-1688.2004.tb01046.x.

Battjes, J. A., and R. J. Labeur. 2017. *Unsteady flow in open channels*. Cambridge, UK: Cambridge University Press.

BBC (British Broadcasting Corporation). 2018. "*Laos dam collapse: Many feared dead as floods hit villages*." *BBC News*, September 3, 2018.

Chanson, H. 2004. *Environmental hydraulics for open channel flows*. Boston: Butterworth-Heinemann.

Chaudhry, M. H. 2007. *Open-channel flow*. New York: Springer.

Chow, V. T. 1988. *Applied hydrology*. New York: McGraw-Hill.

CPRM and ANA (Serviço Geológico do Brasil and Agência Nacional de Águas). 2015. *Monitoramento Especial da Bacia do Rio Doce*. Primeira Campanha de Campo, Acompanhamento da onda de cheia. Belo Horizonte, Brazil: CPRM and ANA.

CPRM and ANA (Serviço Geológico do Brasil–Agência Nacional de Águas). 2016. *Monitoramento Especial da Bacia do Rio Doce*. Quarta Campanha de Campo, Hidrometria, Sedimentometria e Qualidade da Água nas Estações Fluviométricas da RHN após a Ruptura da Barragem de Rejeito. Belo Horizonte, Brazil: CPRM and ANA.

Deltares. 2019. "Delft3D-FLOW—Simulation of multi-dimensional hydrodynamic flows and transport phenomena, including sediments." In *Delft3D—3D/2D modelling suite for integral water solutions—User manual*. Delft, Netherlands: Deltares.

DHI (Danish Hydraulic Institute). 2017. *MIKE 11—A; Channels—Reference manual*. Hørsholm, Denmark: DHI Water & Environment.

DHI (Danish Hydraulic Institute). 2019. "MIKE 21." Accessed March 25, 2019. http://www.mikepoweredbydhi.com/products/mike-21.

DNRC (Dept. of Natural Resources and Conservation). 2018. *Downstream hazard classification procedures for Montana dams*. Helena, MT: Montana DNRC.

Dolce, C. 2019. "Before-and-after images show ongoing flood disaster in Nebraska and Iowa." Accessed March 25, 2019. https://weather.com/news/news/2019-03-17-flooding-before-and-after-images-midwest-nebraska.

Dooge, J. C. I., and B. M. Harley. 1967. "Linear routing in uniform open channels." In *Proc., Int. Hydro Symp.*, 57–63. Fort Collins, CO: Colorado State Univ.

FEMA. 2013. *Federal guidelines for inundation mapping of flood risks associated with dam incidents and failures*. Helena, MT: FEMA.

FLO-2D. 2019. "FLO-2D software | Hydrologic and hydraulic modeling software." Accessed March 25, 2019. https://www.flo-2d.com/.

Flow Science. 2019. "FLOW-3D | We solve the world's toughest CFD problems." Accessed March 25, 2019. https://www.flow3d.com/.

Geonetwork. 2007. "Portal metadados ANA–Geonetwork." Accessed June 23, 2017. http://metadados.ana.gov.br/geonetwork/srv/pt/main.home.

Hayami, S. 1951. *On the propagation of flood waves*, 12–20. Kyoto, Japan: Kyoto Univ.

Julien, P. Y. 2018. *River mechanics*. Cambridge, UK: Cambridge University Press.

Leonard, B. P. 1979. "A stable and accurate convective modelling procedure based on quadratic upstream interpolation." *Comput. Methods Appl. Mech. Eng.* 19 (1): 59–98. https://doi.org/10.1016/0045-7825(79)90034-3.

Mahmood, V., and V. Yevjevich. 1975. *Unsteady flow in open channels*. Fort Collins, CO: Water Resources Publications.

McCuen, R. H. 2016. *Hydrologic analysis and design*. Boston: Pearson.

Moin, P. 2010. *Fundamentals of engineering numerical analysis*. Cambridge, UK: Cambridge University Press.

Morgenstern, N. R., S. G. Vick, C. B. Viotti, and B. D. Watts. 2016. *Report on the immediate causes of the failure of the Fundão dam*. New York: Cleary Gottlieb Steen & Hamilton LLP.

Ostad-Ali-Askari, K., and M. Shayannejad. 2016. "Flood routing in rivers by Muskingum's method with new adjusted coefficients." *Int. Water Technol. J.* 6 (3): 189–194.

Palu, M. C. 2019. "Floodwave and sediment transport assessment along the Doce river after the Fundão tailings dam collapse (Brazil)." Ph.D. thesis, Dept. of Civil and Environmental Engineering, Colorado State Univ.

Palu, M. C., and P. Y. Julien. 2019. "Modeling the sediment load of the Doce River after the Fundão tailings dam collapse, Brazil." *J. Hydraul.*

Eng. 145 (5): 05019002. https://doi.org/10.1061/(ASCE)HY.1943-7900.0001582.
Perdikaris, J., B. Gharabaghi, and R. Rudra. 2018. "Evaluation of the simplified dynamic wave, diffusion wave and the full dynamic wave flood routing models." *Earth Sci. Res.* 7 (2): 14. https://doi.org/10.5539/esr.v7n2p14.
Pilotti, M., A. Maranzoni, L. Milanesi, M. Tomirotti, and G. Valerio. 2014. "Dam-break modeling in alpine valleys." *J. Mt. Sci.* 11 (6): 1429–1441. https://doi.org/10.1007/s11629-014-3042-0.
Ponce, V. M. 2014. *Engineering hydrology.* London: Macmillan Education.
Price, R. K. 2009. "Volume-conservative nonlinear flood routing." *J. Hydraul. Eng.* 135 (10): 838–845. https://doi.org/10.1061/(ASCE)HY.1943-7900.0000088.
Reuters. 2018. *Myanmar dam breach floods 85 villages, thousands driven from homes*. London: Reuters.
Roberson, J. A., J. J. Cassidy, and M. H. Chaudhry. 1998. *Hydraulic engineering*. New York: Wiley.
Rowinski, P., and A. Radecki-Pawlik. 2015. "Rivers–Physical, fluvial and environmental processes." In *GeoPlanet: Earth and planetary sciences*. Dordrecht, Netherlands: Springer.
Sturm, T. W. 2009. *Open channel hydraulics*. New York: McGraw-Hill.
Sylvestre, J., D. L. Fread, and J. M. Lewis. 2010. *FLDWAVE MODEL: River mechanics group*. Silver Spring, MD: River Mechanics.net.
Szymkiewicz, R. 2010. *Numerical modeling in open channel hydraulics*. New York: Springer.
TELEMAC. 2019. "Open TELEMAC-MASCARET." Accessed March 25, 2019. http://www.opentelemac.org/.
USACE. 2016c. *HEC-RAS–River analysis system–2D Modeling user manual version 5.0*. Davis, CA: Hydrologic Engineering Center.
USACE. 2016d. *HEC-RAS User's manual*. Davis, CA: Hydrologic Engineering Center.
USBR (US Bureau of Reclamation). 2017. "Technical service center|Bureau of reclamation intranet." Accessed March 25, 2019. https://www.usbr.gov/tsc/techreferences/computer%20software/models/srh2d/index.html.
USBR (US Bureau of Reclamation). 2018. "Technical service center|Bureau of reclamation intranet." Accessed March 25, 2019. https://www.usbr.gov/tsc/techreferences/computer%20software/models/srh1d/index.html.
USDA. 2014. "Chapter 17–Flood routing." In *Hydrology national engineering handbook*. Washington, DC: USDA.
USSD (US Bureau Society on Dams). 2018. *Independent forensic team report Oroville dam spillway incident*. Sacramento, CA: Incident Independent Forensic Team.
Wu, W. 2007. *Computational river dynamics*. London: CRC Press.
Zijlema, M. 2015. "*Computational* modelling *of flow and transport*." In *Lecture notes*. Delft, Netherlands: Delft Univ. of Technology.